Electrochimica Acta 331 (2020) 135255

Contents lists available at ScienceDirect

Electrochimica Acta

journal homepage: www.elsevier.com/locate/electacta

Decoupled electrolysis using a silicotungstic acid electron-coupled-proton buffer in a proton exchange membrane cell

Greig Chisholm, Leroy Cronin**, Mark D. Symes*

WestCHEM, School of Chemistry, University of Glasgow, Glasgow, G12 8QQ, United Kingdom

ARTICLE INFO

Article history:
Received 14 September 2019
Received in revised form
8 November 2019
Accepted 8 November 2019
Available online 13 November 2019

Keywords:
Oxygen evolution reaction
Mediated electrolysis
Decoupled electrolysis
Electron-coupled-proton buffer
Polyoxometalate

ABSTRACT

The storage of renewably-generated energy as hydrogen *via* the electrolysis of water is a fundamental cornerstone of a sustainable hydrogen economy. Conventional electrolysers usually require stable power inputs in order to operate effectively and safely and so may be unsuited to harnessing renewable power, which is often intermittent and diffuse. Electrolysis mediated by Electron-Coupled-Proton Buffers has the potential to overcome some of the challenges surrounding electrolysis using low and/or sporadic power inputs (especially those related to gas crossover) as the use of Electron-Coupled-Proton Buffers allows the oxygen and hydrogen evolution reactions to be completely decoupled from one another. Herein, we show that silicotungstic acid can be used as an Electron-Coupled-Proton Buffer in a proton exchange membrane cell, decoupling the hydrogen and oxygen evolution reactions at steady state current densities as high as 500 mA cm^{-2}. O_2 and H_2 can be produced continuously by this system by cycling a fixed volume of the Electron-Coupled-Proton Buffer solution. Even at current densities as low as 25 mA cm^{-2}, the level of hydrogen in the oxygen stream is <0.4%, whereas a conventional proton exchange membrane electrolyser operating at this current density produces oxygen containing nearly 2% hydrogen (unacceptable for most applications). Furthermore, using silicotungstic acid as an Electron-Coupled-Proton Buffer also confers greater tolerance to non-deionised water inputs and reduces fluoride release from the perfluorosulfonated membrane (a marker for membrane degradation) relative to a conventional proton exchange membrane electrolyser. Together, these results highlight the promise and potential advantages of Electron-Coupled-Proton Buffers (and silicotungstic acid in particular) for the electrolytic production of hydrogen and oxygen over a wide range of current densities, such as might be delivered by renewable power inputs.

1. Introduction

The electrolysis of water to generate hydrogen and oxygen is seen as an increasingly attractive route by which to store intermittent, renewably-generated electricity, as hydrogen is an excellent transportable fuel [1–3]. Consumption of this fuel (either by combustion or in an electrochemical device such as a fuel cell) releases only energy and water, meaning that electrolytically-generated hydrogen has tremendous potential as a sustainable energy vector [4,5]. Significant challenges remain, however, for the large-scale electrolytic production of H_2 using renewable power inputs, not least because conventional electrolysers do not function well when driven by intermittent and/or low power inputs, which tend to characterise renewables [6–9]. For example, at low current densities, the rates at which H_2 and O_2 are produced in an electrolyser may in fact be slower than the rates at which these gases permeate the membrane [10]. Such gas crossover would, at the very least, reduce the amount of hydrogen that could be harvested from such a device and hence the efficiency of electrolysis, and could in extreme cases lead to the creation of hazardous mixtures of hydrogen and oxygen. Gas crossover of this nature would also be expected to lead to the production of reactive oxygen species that degrade cell components (in particular the membrane) and hence shorten the electrolyser's lifespan [11,12].

Against this backdrop, we recently began exploring the concept of decoupled electrolysis [13–15], whereby the oxygen evolution reaction is coupled to the simultaneous reversible reduction and protonation of a redox mediator (rather than to the reduction of

* Corresponding author.
** Corresponding author.
E-mail addresses: lee.cronin@glasgow.ac.uk (L. Cronin), mark.symes@glasgow.ac.uk (M.D. Symes).

https://doi.org/10.1016/j.electacta.2019.135255

protons to H_2). Subsequent re-oxidation of the redox mediator then provides the necessary electrons and protons to drive the hydrogen evolution reaction, which can take place at an entirely different time and in an entirely different place to the oxygen evolution step [16]. On account of their ability to reversibly store both protons and electrons, such mediators are known as Electron-Coupled-Proton Buffers (ECPBs). When using an ECPB, the rate of the hydrogen evolution reaction depends on the rate of re-oxidation of the redox mediator, rather than the rate of the oxygen evolution reaction. The two half-reactions of water splitting can thus be considered to be *decoupled* from each other, inasmuch as the current for the oxygen evolution reaction need not bear any particular relationship to the current for any subsequent hydrogen evolution reaction (in contrast to coupled electrolysis, where the oxidation of water proceeds with concomitant reduction of protons and so the currents for these processes must necessarily be the same). Since our initial reports, the concept of decoupled electrolysis has subsequently been elaborated upon, both by ourselves [17–24] and others [25–40].

Amongst the various redox mediators that have been suggested for such decoupled electrolysis, the polyoxometalate silicotungstic acid ($[H_4SiW_{12}O_{40}]$) presents considerable scope for future applications on account of its robustness and the position of its redox waves. At pH 0.5, this polyoxometalate possesses two reversible 1-electron redox waves with $E_{1/2} = +0.01$ V and -0.22 V *vs.* NHE respectively [41]. This means that both reductions can be performed on a carbon electrode in aqueous solution without any concomitant hydrogen evolution activity (H_2 evolution on carbon is not appreciable at potentials more positive than -0.6 V), but that subsequent exposure of the two-electron reduced species $H_6[SiW_{12}O_{40}]$ to a catalyst such as platinum will lead to spontaneous hydrogen evolution until equilibrium between H_2 and reduced mediator is reached [17]. In practice, this means that after contacting a fully two-electron reduced mediator with a suitable catalyst, an equilibrium mixture of $H_4[SiW_{12}O_{40}]$ and the 1-electron reduced form, $H_5[SiW_{12}O_{40}]$ is obtained, as the $E_{1/2}$ value for this couple (+0.01 V) is almost exactly the same as for proton reduction at this pH. Indeed, it was also observed that a mixture of $H_4[SiW_{12}O_{40}]$ and $H_5[SiW_{12}O_{40}]$ could be produced by exposing $H_4[SiW_{12}O_{40}]$ to hydrogen gas in the presence of a suitable catalyst [17]. Moreover, this same study established that the two-electron reduced form of the mediator, $H_6[SiW_{12}O_{40}]$, spontaneously reacts with oxygen and so has the ability to remove dissolved oxygen from solution, which could be useful for the prevention of formation of reactive oxygen species in any decoupled electrolysis device employing this polyoxometalate.

Our previous study of silicotungstic acid as an ECPB was conducted entirely batch-wise in glassware, using small-area electrodes inserted into wide-gap H-cells in which resistive losses were high [17]. In order to more properly assess the potential advantages and disadvantages of a decoupled electrolysis system based on this mediator, it is necessary to move towards a more carefully engineered back-to-back configuration with flowed anolyte and catholyte feeds. Herein, we report the construction and optimisation of the electrochemical part of this system, wherein water is oxidised to generate oxygen and the ECPB is reduced and protonated. Through the use of a second electrochemical cell to re-oxidise the reduced ECPB, we show that this system can almost completely decouple (by 99%) the oxygen and hydrogen evolution reactions from each other under continuous and stable steady-state operation at an imposed current density of 500 mA cm^{-2}, with cell voltages only a little in excess of 2 V. We then go on to show that such a system allows the production of oxygen at current densities as low as 25 mA cm^{-2} without hazardous levels of hydrogen being evident in the oxygen product, in contrast to the behaviour of a conventional proton exchange membrane electrolyser operating under analogous conditions. This validates one of the key claims made for decoupled electrolysis (that it allows that production of the product gases of electrolysis in a safe manner under very low power inputs, such as might be delivered by renewable energy sources). Moreover, we then show that the suppression of hydrogen production inside the electrochemical cell brought about by the high level of decoupling might also lead to a lower rate of membrane degradation relative to that observed in a conventional proton exchange membrane electrolyser. This study therefore forms an important milestone in developing the applications of decoupled electrolysis.

2. Materials and methods

2.1. Materials and general methods

Sodium bicarbonate, potassium sulfate, calcium nitrate and magnesium chloride were purchased from Sigma Aldrich. All chemical reagents were used as purchased. All aqueous solutions were prepared with ultrapure grade water (18.2 MΩ-cm resistivity), unless otherwise stated. All other materials were obtained as stated in the text. All electrochemical data were collected using a BioLogic SP-150 potentiostat coupled to a BioLogic VMP-3B 20A booster. Data were collected and analysed using the EC-Lab software (BioLogic, version 10.40).

2.2. Electrolysis system design and construction

A general schematic of the set-up used in this work is shown in Fig. 1.

The oxygen-producing electrochemical cell was constructed as follows: the anode of this cell consisted of a 10 mm-thick titanium serpentine flow field utilising 6 parallel flow channels of 1 mm^2 cross-section and a platinised titanium mesh (supplied by Fuelcellsetc). These elements were sealed using a 0.1 mm-thick polytetrafluoroethylene (PTFE) gasket (Labtex). The cathode consisted of a 10 mm-thick titanium serpentine flow field as described above and a layer of TGP-H60 carbon paper (Alfa Aesar). Prior to insertion of the cathodic flow plate into the cell, the flow fields of the plate were immersed in Aqua Regia for 90 min. This ensured a completely clean surface and minimised any parasitic cathodic hydrogen generation. These elements were sealed using a 0.15 mm-thick cellulose fibre gasket (Klinger, AE5057613). The anode and cathode were separated by a Nafion 117-based catalyst-coated membrane supplied by Ion Power. This membrane was coated with IrO_2 (1 mg/cm^2) (anode side, producing oxygen). No catalyst was applied to the cathode side (reducing the ECPB). The active area of the membrane was 12.96 cm^2. The anode and cathode were compressed against the membrane *via* 10 mm-thick PTFE insulating plates and 10 mm-thick aluminium end plates. The bolts fastening the cells were tightened to a torque of 5 Nm. Prior to all experiments, the catholyte loop and reservoir were sparged with argon for 30 min at a flow rate of 300 mL/min.

The electrochemical cell for re-oxidation of the reduced ECPB was constructed from similar components to those used for the oxygen-generating cell as follows. The anode of this cell consisted of a 3 mm-thick titanium serpentine flow field, and a layer of TGP-H60 carbon paper. These elements were sealed using a 0.15 mm-thick cellulose fibre gasket. The cathode consisted of a 3 mm-thick titanium serpentine flow field and a layer of TGP-H60 carbon paper. These elements were sealed using a 0.15 mm-thick cellulose fibre gasket. The anode and cathode were separated by a Nafion 117-based catalyst-coated membrane supplied by Ion Power. This membrane was coated with Pt (0.3 mg/cm^2) (cathode side, for

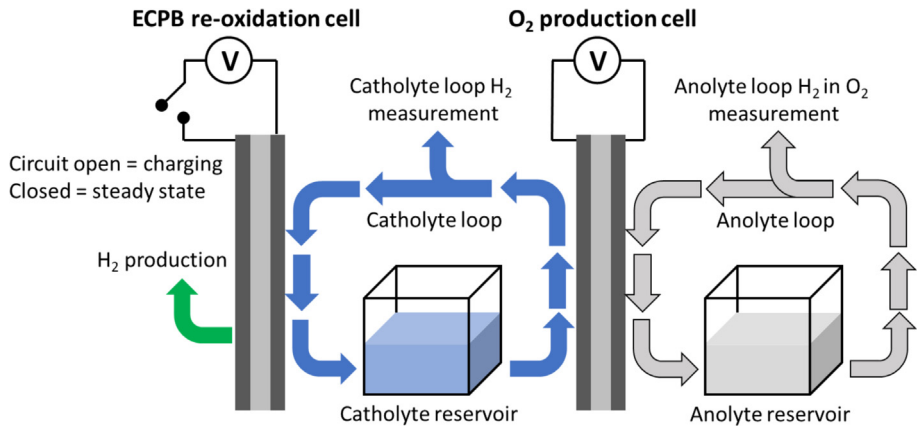

Fig. 1. A schematic of the device set-up used in this work. A full description of materials and construction is given in the text.

hydrogen generation). No catalyst was applied to the anode side (ECPB re-oxidation). The active electrode area of this membrane electrode assembly was 12.96 cm^2. The anode and cathode were compressed against the membrane *via* 10 mm-thick PTFE insulating plates and 10 mm-thick aluminium end plates. The bolts fastening the cells were tightened to a torque of 5 Nm.

2.3. Configuration of standard PEM electrolyser

For comparison between coupled and decoupled electrolysis, a conventional Proton Exchange Membrane (PEM) electrolyser was constructed as follows. The anode of this cell consisted of a 3 mm-thick titanium serpentine flow field and a platinised titanium mesh. These elements were sealed using a 0.1 mm-thick PTFE gasket. The cathode consisted of a 3 mm-thick titanium serpentine flow field and a layer of TGP-H60 carbon paper. These elements were sealed using a 0.15 mm-thick cellulose fibre gasket. The anode and cathode were separated by a Nafion 117-based catalyst-coated membrane supplied by Ion Power. This membrane was coated with IrO_2 (1 mg/cm^2) (anode side) and platinum (0.3 mg/cm^2) (cathode side). The active area of the membrane was 12.96 cm^2. The anode and cathode were compressed against the membrane *via* 10 mm-thick PTFE insulating plates and 10 mm-thick aluminium end plates. The bolts fastening the cells were tightened to a torque of 5 Nm. Unless stated otherwise, ultra-pure water (18.2 MΩ-cm resistivity) was pumped through the anode of this electrochemical cell at a rate of 40 mL min^{-1}. The temperature of the water reservoir was maintained using an oil bath such that the temperature of the water entering the cell was 30 °C. A gas outlet from this anolyte reservoir was connected to the auto-sampling port of the gas chromatography machine (see below) to monitor gas compositions as a function of operational parameters. A current potential curve was obtained for this cell to test its operation (Fig. 2). This curve was obtained by stepping the voltage in 100 mV steps at 10 min intervals. The average current was measured across the last 5 min of each interval. The performance of the electrolyser was comparable to that of proton exchange membrane electrolysers of similar construction at similar temperatures reported in the literature [42–44].

2.4. Quantifying decoupling of the oxygen and hydrogen evolution reactions

The extent of parasitic hydrogen evolution on the cathode side of the cell during reduction of the ECPB was gauged by collecting the hydrogen gas generated in a gas burette. The number of moles

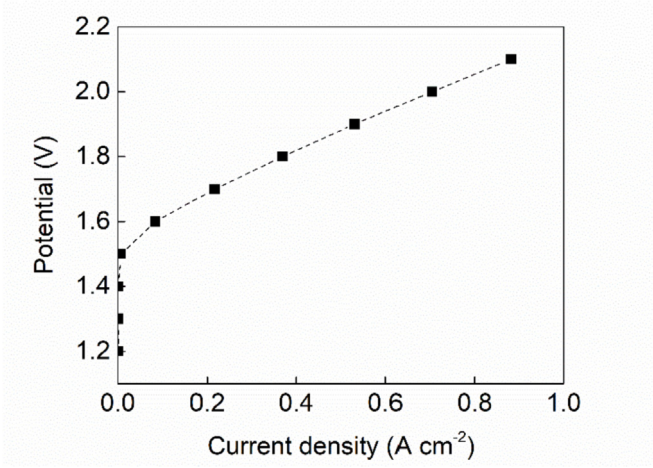

Fig. 2. Current-potential curve for the conventional proton exchange membrane electrolyser used as a comparison to the ECPB-mediated system.

of hydrogen to which this volume equated was then calculated by taking the volume of 1 mol of an ideal gas at room temperature and pressure to be 24.5 L. This number of moles was then compared to the number of moles of hydrogen that could theoretically have been produced if all the charge passed during the reduction reaction had been used in driving the hydrogen evolution reaction (instead of ECPB reduction). This theoretical (0% decoupling) number of moles of hydrogen was obtained by dividing the charge passed during the electrolysis by 2*F* (where *F* is the Faraday constant). The efficiency of decoupling (as a %) is then obtained by applying the formula:

$$Decoupling\ Efficiency = 1 - \frac{moles\ of\ hydrogen\ detected}{theoretical\ maximum\ moles\ hydrogen} \times 100$$

2.5. Quantifying hydrogen levels in the oxygen stream

The oxygen stream from the anode side of the cells was routed through an Agilent Technologies 7890A gas chromatography (GC) system (equipped with a thermal conductivity detector) *via* a pneumatically-operated automatic gas sampling valve. The cells were connected to the GC system using 316 stainless steel tubing of

$^1/_8$ inch internal diameter. An Agilent 19041P-MS4 column was used (dimensions = 30 m × 320 μm × 12 μm) at a flow rate of 0.45108 mL min^{-1}, and a pressure of 2.8504 psi. The GC oven temperature was set to 27 °C and no carrier gas was used. The GC system was calibrated for H_2 using certified standards of hydrogen at a range of volume % in argon supplied by CK Gas Products Limited (UK). Linear fits of volume % *vs.* peak area were obtained, which allowed peak areas to be converted into volume % of H_2 in the measured gas.

2.6. Determination of electrolyte fluoride content

Electrolyte fluoride content was measured using a perfectION™ ion specific fluoride electrode from Mettler Toledo. Calibration of the electrode was carried out using a low level "Total Ionic Strength Adjustment Buffer" (TISAB) prepared as follows: 500 mL of deionised water was added to a 1 L beaker. 57 mL of glacial acetic acid was added followed by 58 g of sodium chloride. The pH of this solution was adjusted to 5.0–5.5 using an aqueous 5 M NaOH solution. 25 mL of a standard fluoride solution was prepared using 250 μL of 1000 mg/mL fluoride standard (supplied by Mettler Toledo) and 18.2 MΩ-cm water. A calibration standard solution was then prepared using 18.2 MΩ-cm water (25 mL) and low level TISAB solution (25 mL). Volumes were measured accurately using a graduated pipette. The electrode potential was then plotted versus the log of the fluoride concentration for each calibration standard. The resulting calibration curve gave a linear relationship between the log of the fluoride concentration and the electrode potential. The R^2 for this calibration was typically >0.98.

3. Results and discussion

3.1. Optimisation of steady state electrolysis conditions

A system as shown in Fig. 1 was constructed, using an aqueous solution of fully-oxidised silicotungstic acid (0.25 M) for both the anode and cathode feeds in order to balance the osmotic pressure across the membrane. The flow rate in for the anode feed (performing water oxidation in the presence of oxidised polyoxometalate) was set to 40 mL min^{-1}, whilst the cathode feed flow rate (performing polyoxometalate reduction in competition with hydrogen evolution) was initially set to 250 mL min^{-1}. The temperatures of the reservoirs for both feeds were maintained using oil baths such that the temperatures of the feeds as they entered the cell were both 30 °C.

The state of charge of the catholyte solution was then increased to 100% (corresponding to complete reduction of the polyoxometalate in the catholyte solution by one electron) by controlled current electrolysis at 1.296 A (100 mA cm^{-2}) across the O_2-production cell. During this time, the circuit on the ECPB re-oxidation cell was left open so that no re-oxidation of the ECPB occurred. The ECPB became progressively more reduced during this charging process, but no H_2 was ever detected in the cathode loop, suggesting complete decoupling was achieved during charging. A representative plot of applied voltage and state of charge of the ECPB versus time for this charging process is shown in Fig. 3.

The elongated "S" shape in the voltage-time curve in Fig. 3 is characteristic of this charging process, with a steady increase in voltage as the concentration of silicotungstic acid available for reduction is depleted. There is then a plateau in voltage as the state of charge reaches 100%, signalling that all the polyoxometalate is reduced by one electron and that the second reduction process is beginning.

After charging to 100% (corresponding to complete reduction of all the polyoxometalate in the cathode loop by one electron per

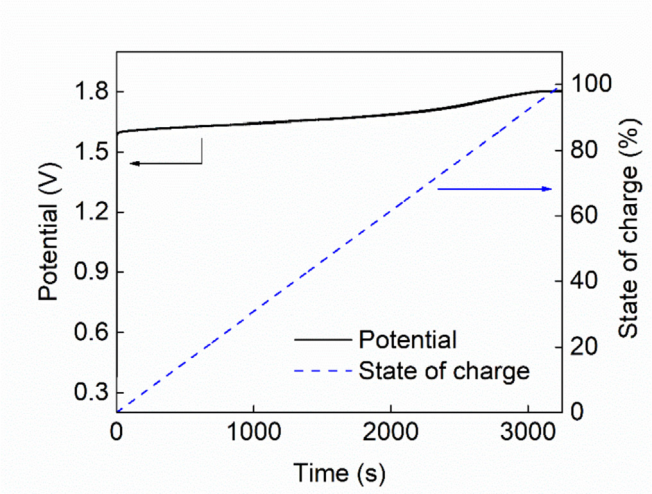

Fig. 3. Voltage-time (black solid line) and state-of-charge (blue dashed line) curves for the charging of the catholyte in the ECPB electrolyser to a 100% state-of-charge (every silicotungstic acid molecule reduced by one electron). Operational parameters are given in the text.

polyoxometalate molecule), the circuit on the ECPB re-oxidation cell was closed, allowing re-oxidation of the polyoxometalate. By setting the imposed current density across this ECPB re-oxidation cell to the same value as that imposed across the oxygen production cell, the system could then be placed into steady state. We note here that although the reduced silicotungstic acid ECPB can be re-oxidised spontaneously in a non-electrochemical catalytic reaction (generating hydrogen without an applied potential as in our previous report [17]), the system under discussion in this paper employs electrochemical re-oxidation as that was found to be the simplest way in which to place the system into a controlled steady state and hence monitor accurately the performance of the water oxidation and ECPB reduction electrochemical cell. The voltages across the oxygen-producing cell required to maintain steady state current densities of 100, 250 and 500 mA cm^{-2} were then measured, as shown in Table 1. Fig. 4 shows an example voltage-time curve for one such steady state experiment, where charge in excess of five times that required to fully reduce the polyoxometalate by two electrons was passed after the system was placed into steady state (without altering the overall state-of-charge of the mediator, as gauged by subsequent re-oxidation of the ECPB), demonstrating that a steady state of ECPB reduction and re-oxidation was reached.

At the end of each experiment, the ECPB in the catholyte loop was fully re-oxidised by application of a voltage to the ECPB re-oxidation electrochemical cell only. The number of coulombs required for complete re-oxidation was measured and compared to the number of coulombs used in the initial charging process. This gives a "Final state of charge" value (where 100% indicates that the state of charge after the steady state experiment is exactly the same

Table 1
Cell voltages and decoupling percentages at a range of steady state current densities at an ECPB concentration of 0.25 M, at 30 °C with an anolyte flow rate of 40 mL min^{-1} and a catholyte flow rate of 250 mL min^{-1}.

Current Density	100 mA/cm^2	250 mA/cm^2	500 mA/cm^2
Initial state of charge (%)	100	100	100
Final state of charge (%)	105	93	99
Decoupling (%)	97	98	76
Cell voltage (V)	1.85	2.01	2.35

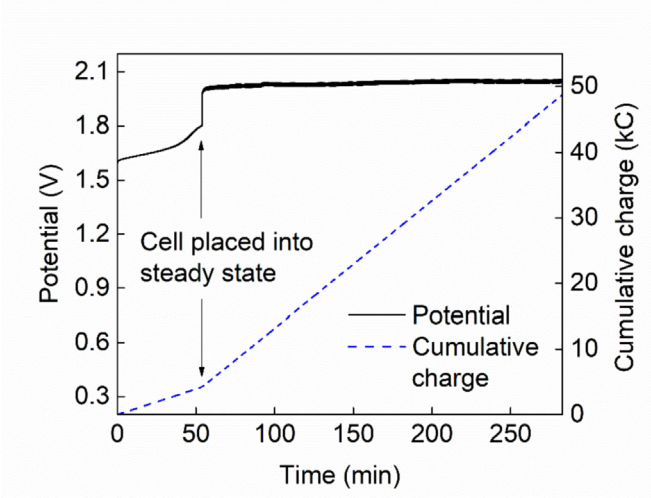

Fig. 4. Example voltage-time curve for the charging of the catholyte solution at a current density of 100 mA cm^{-2}, followed by steady-state operation at 250 mA cm^{-2}. In the initial charging step, 4240 C were transferred. After placing into steady state (indicated by the arrows in the figure) an additional 44,164 C were passed. After this steady state operation, the catholyte was re-oxidised and the 4240 C used in the initial reduction were recovered (data not shown).

as that at the beginning), which gives an indication as to the degree to which the process was operating at a steady state during the test. The variations in starting and final charge in Table 1 all suggest that the system is operating at steady state under these conditions. Furthermore, the volume of hydrogen production in the cathode loop (an unwanted parasitic side-reaction to ECPB reduction) was also measured to give a measurement of the effectiveness of silicotungstic acid as a mediator for decoupled electrolysis under these steady state conditions. As shown in Table 1, this "Decoupling %" (see Section 2.4 for definition) is very high at 100 and 250 mA cm^{-2} (indicating very little parasitic hydrogen production), but this value falls off considerably at the higher current density of 500 mA cm^{-2}.

In an attempt to improve the extent of ECPB-mediated decoupling of the oxygen and hydrogen evolution reactions at high current densities, the concentration and flow rate of the catholyte feed were varied (the anolyte flow rate was maintained at 40 mL min^{-1} in all experiments). Working on the hypothesis that the low % decoupling observed at higher current densities was due to depletion of the ECPB at the cathode of the oxygen-producing cell (leading to an increase in parasitic hydrogen evolution in order to maintain the imposed current density), the concentration of silicotungstic acid in the catholyte solution was increased to 0.4 M. The concentration of the anolyte feed was also increased to 0.4 M in order to maintain the osmotic balance across the membrane. The effects of increasing the concentration of silicotungstic acid in this way are summarised in Table 2, which also shows that increasing the catholyte flow rate from 250 mL min^{-1} to 500 mL min^{-1} leads to a small reduction in the required cell voltage under an imposed current density of 250 mA cm^{-2}.

These data show that increasing the ECPB concentration and catholyte feed flow rate have only very marginal effects on the cell voltage and % decoupling at a current density of 250 mA cm^{-2}, but significantly improve both metrics at the higher current density of 500 mA cm^{-2}, leading to 99% decoupling at a silicotungstic acid concentration of 0.4 M and a flow rate of 500 mL min^{-1}. In this way, it can be seen that effectively complete decoupling of the hydrogen and oxygen evolution reactions can be achieved using silicotungstic acid as a mediator, even at steady-state current densities as high as 500 mA cm^{-2}. Meanwhile, Table 2 also shows a comparison to a conventional electrolyser (see Section 2.3) performing entirely coupled oxygen and hydrogen evolution. Hence, at 500 mA cm^{-2}, there is an approximate 300 mV penalty for decoupling the hydrogen and oxygen evolution reactions using silicotungstic acid as a mediator.

Table 2
The effect of ECPB concentration and flow rate on cell voltages and decoupling percentages at 30 °C at a range of steady state current densities.

Current Density (mA cm^{-2})	250	250	250	500	500	500[a]
[ECPB] (M)	0.25	0.4	0.4	0.25	0.4	0
Catholyte flow rate (mL min^{-1})	250	250	500	250	500	N/A
Decoupling (%)	98	100	100	76	99	0
Cell voltage (V)	2.01	1.99	1.92	2.35	2.16	1.85

[a] A conventional electrolyser operating using 18.2 MΩ-cm water with no catholyte and with an anode feed flow rate of 40 mL min^{-1} (the same as for the ECPB system).

3.2. Comparison of conventional and ECPB-Mediated electrolysis at low current densities

The above results relate to operation at comparatively high current densities. However, one of the chief advantages of an ECPB-mediated system is that it should, at least in theory, allow water splitting to occur at much lower current densities (such as might be delivered by diffuse renewable power sources) without significant mixing of the product gases as the gases are not made in the same cell at the same time [16,17]. In order to test this hypothesis in our silicotungstic acid-mediated system, we conducted low-current density electrolysis of water in a conventional electrolyser and compared the purity of the oxygen generated by this cell with that obtained from our ECPB-mediated system.

Current densities of 25 and 50 mA cm^{-2} were probed for both the conventional and ECPB-mediated systems. For both systems, the anode feeds were circulated at 40 mL min^{-1}. There was no cathode feed for the conventional electrolyser, which was instead equipped with a gas outlet to allow hydrogen to escape. The flow rate for the catholyte feed for the ECPB-mediated electrolyser was maintained at 250 mL min^{-1}. The temperature for both systems was maintained at 30 °C, and the purity of the oxygen generated at the anode side of the cells was gauged by gas chromatography (see Section 2.5). The ECPB catholyte feed was charged to a state of charge of 105% before the experiment was initiated (corresponding to complete reduction of the polyoxometalate by one electron, with 5% of the polyoxometalate molecules reduced by a second electron as well) and then maintained at steady state during the subsequent electrolysis. The % H_2 in the anode oxygen product stream was monitored over the course of 16 h (see Table 3) and the percentages of H_2 detected are quoted as averages of at least five measurements in each case.

A general regulatory rule-of-thumb is that any process involving mixtures of hydrogen in oxygen should aim to maintain a hydrogen concentration in oxygen below 0.4% (10% of the lower explosion limit of hydrogen in oxygen), with H_2 levels up to 25% of this lower explosion limit (*i.e.* a 1% mixture of H_2 in O_2) allowed only on an

Table 3
The percentage of hydrogen in the anolyte oxygen product stream as a function of current density at 30 °C for a conventional and ECPB-mediated electrolyser.

Current Density (mA cm^{-2})	% H_2 in O_2 stream	
	Conventional electrolyser	ECPB-mediated electrolyser
25	1.89 (±0.02)	0.31 (±0.07)
50	1.47 (±0.04)	0.31 (±0.04)

occasional and temporary basis [45]. Levels of hydrogen in oxygen above this limit, or above 0.4% for extended periods of time, are deemed unsafe. Hence the data in Table 3 show that a conventional electrolyser operating at 25 or 50 mA cm^{-2} under our conditions would be in breach of these regulatory guidelines, whereas an ECPB-mediated system has the potential to allow safe water electrolysis (% H_2 in O_2 < 0.4%) to proceed even at current densities as low as 25 mA cm^{-2}.

3.3. Comparison of conventional and ECPB-Mediated electrolysis using non-deionised feeds

A conventional proton exchange membrane electrolyser relies on the proton conductivity of its perfluorosulfonated membrane to operate. The presence of other metallic cations can poison this membrane, as the protons in the sulfonate $R{-}SO_3^-H^+$ units exchange for these metal ions (M^+) forming $R{-}SO_3^-M^+$ species, which in turn leads to a dramatic increase in the resistance of the electrochemical cell [46]. In order to prevent such an exchange of protons for other cations in the membrane, a conventional proton exchange membrane electrolyser must therefore use extensively deionised water. If a membrane becomes deactivated due to the presence of alkali metal or other cations, then it is usually possible to recover the performance by treating the membrane in acid in order to exchange the extraneous cations for protons. However, this process is time-consuming and not conducive to continuous operation with non-deionised water.

In contrast, a silicotungstic acid-mediated electrolysis system requires an acidic catholyte feed. Whilst this has the disadvantage of requiring a pump to flow it through the cell (whereas a conventional electrolyser simply has a gas outlet on the cathode side), the acidic ECPB medium should provide a ready route for the removal of cations from the cathode side of the membrane, potentially improving the tolerance of the cell to excursions from ideal water quality. To test this hypothesis, we prepared a standard mineralised water (identical to the cation concentration quoted for Evian mineral water), consisting of 6.5 mg of sodium bicarbonate, 1.0 mg of potassium sulfate, 80 mg of calcium nitrate and 26 mg of magnesium chloride per litre, and used this as the basis of a "mineralised anode feed" for both our conventional and ECPB-mediated electrolysers. The conductivity of this mineralised solution was measured, and was found to be 708 μS/cm.

To this end, our conventional electrolyser was firstly operated using 18.2 MΩ-cm water at 30 °C with an anolyte flow rate of 40 mL min^{-1} at an imposed current density of 500 mA cm^{-2} for 60 min. During this time, the required cell voltage was roughly constant at around 1.9 V. After this time period, the experiment was paused and the anolyte feed was switched to the mineralised water described above. The voltage requirement to maintain this current density rose immediately and dramatically, causing the galvanostat to trip (a rate of voltage increase of 950 mV/h was recorded). The first derivative of the voltage *vs.* time for this experiment is plotted in Fig. 5A (with an expansion in Fig. 5B), in which it can be seen that the rate of change in the voltage was constant until the transition to mineralised water was made. This demonstrates that a conventional electrolyser struggles to handle anything other than very pure water input streams.

In order to test the response of the ECPB-mediated electrolyser to this mineralised water feed, 0.25 M solutions of silicotungstic acid were made up in both 18.2 MΩ-cm water and the mineralised water detailed above. The temperature of the electrolytes entering the electrochemical cell was maintained at 30 °C and the flow rates of the anolyte and catholyte were 40 mL min^{-1} and 250 mL min^{-1} respectively. Again beginning with the 18.2 MΩ-cm based electrolytes for both the anolyte and catholyte, the catholyte was first charged to 100% state-of-charge and then placed into steady state at an imposed current density of 250 mA cm^{-2} in for 1 h. During this time, the voltage requirement was stable and in line with the metrics reported in Tables 1 and 2. After this time, the anolyte solution was replaced with a fresh 0.25 M silicotungstic acid solution prepared using the mineralised water described above (Fig. 5A). In contrast to the behaviour of the conventional proton exchange membrane electrolyser, the ECPB-mediated electrolyser was able to maintain a current density of 250 mA cm^{-2} under these conditions, with only a comparatively modest rate of increase in the required voltage (15–20 mV/h). The ECPB-mediated electrolyser thus seems to be far more resilient (at least over the time-course of a few hours) to the presence of metal cations in the electrolyte than a conventional proton exchange membrane electrolyser. Experiments examining the longer-term effects of using such non-deionised water in ECPB-mediated electrolysis are ongoing. The performance of this silicotungstic acid-mediated electrolyser is compared to the performance of other continuous-flow systems for decoupling the electrochemical oxygen evolution reaction from hydrogen evolution in Table 4.

3.4. Comparison of membrane durability in conventional and ECPB-Mediated electrolysis

In a conventional proton exchange membrane electrolyser, one of the chief routes to membrane degradation is through attack by reactive oxygen species that form in the presence of H_2/O_2 mixtures

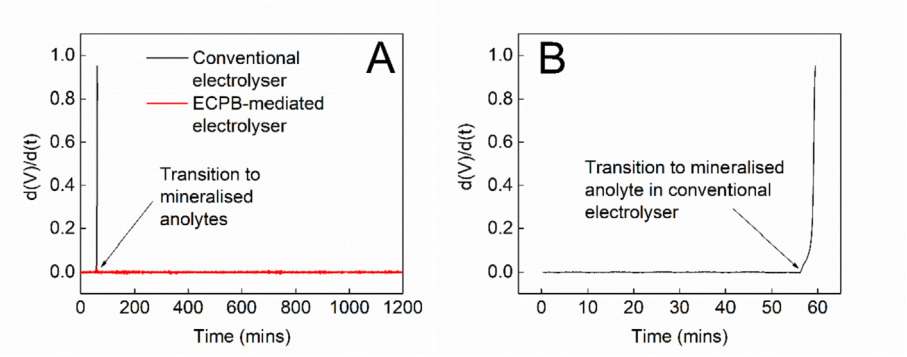

Fig. 5. A: Comparison of the performance of a conventional proton exchange membrane electrolyser (black line) and an ECPB-mediated electrolyser (red line) on moving from a demineralised to a mineralised anolyte feed. The data collection was paused at the point of transition of anolytes in both cases (indicated by the arrow) and recommenced once transition was complete. Hence transition times are not included in the graph. 5B: An expansion of the d(V)/d(t) curve for the conventional proton exchange membrane electrolyser from panel A.

Table 4
A comparison of the electrolysis system reported in this paper to other mediated continuous-flow systems for decoupling the electrochemical oxygen evolution reaction from hydrogen evolution. A "-" symbol in the table below indicates that this data is not given in the corresponding publication.

Entry	Mediator	Max. steady state current density (mA cm^{-2})	% H_2 in O_2	Feedwater purity	Ref.
1	Anthraquinone-2,7-sulfonic acid	250	None [a]	18.2 MΩ-cm	22
2	$[P_2W_{18}O_{62}]^{6-}$	50	–	18.2 MΩ-cm	23
3	$H_6ZnW_{12}O_{40}$	30	–	–	24
4	Ce(III)/Ce(IV)	80	–	18.2 MΩ-cm	25
5	$H_4SiW_{12}O_{40}$	500	0.31	Mineralised feeds tolerated	This work

[a] The report states that no hydrogen was detected in the oxygen stream, but no detection limit is quoted.

[11,47,48]. In the case of Nafion (currently the membrane of choice for proton exchange membrane electrolysers), the degradation of the membrane can be gauged by monitoring the concentration of fluoride in the solution emerging from the electrochemical cell as a proxy for membrane degradation [49,50]. However, in an ECPB-mediated cell using silicotungstic acid, almost no H_2 is produced in the water-oxidising electrolytic cell. This vastly reduces hydrogen cross-over into the anode side of the cell (see Section 3.2) and hence the likelihood of reactive oxygen species forming on the anode side of this cell. Hence we hypothesised that the use of silicotungstic acid as an ECPB should help to reduce the formation of reactive oxygen species that form as a consequence of gas cross-over, and hence lead to slower rates of membrane degradation.

In order to test this hypothesis, a conventional electrolyser was constructed as before (Section 2.3) and ultra-pure water (18.2 MΩ-cm) was pumped through the anode of this electrochemical cell at a rate of 40 mL min^{-1} at a constant temperature of 30 °C. The durability of the membrane was then tested by running the electrolyser at a current density of 100 mA cm^{-2} for 200 h. Samples for fluoride concentration analysis (see Section 2.6) were taken periodically by combining any condensate from the hydrogen gas stream with the anode water reservoir, thoroughly mixing and withdrawing a 25 mL sample using a graduated pipette. Prior to analysis, this 25 mL sample was combined with 25 mL of low level TISAB solution (see Section 2.6). In the following calculations, correction has been made to take into account any apparent increase in fluoride concentration that might manifest as a consequence of the reduction in volume of the water in the anode loop due to electrolysis. As shown in Fig. 6A, the concentration of fluoride in the samples collected from the conventional electrolyser increases considerably over the course of the experiment, reaching 0.5 mg L^{-1} after 200 h.

The performance of an ECPB-mediated system at steady state and at 30 °C was then evaluated. In this system, the anolyte was again fully oxidised 0.25 M aqueous silicotungstic acid (flow rate = 40 mL min^{-1}), whilst the catholyte was 0.25 M aqueous silicotungstic acid at a 105% state of charge (flow rate = 250 mL min^{-1}). Samples were taken periodically from both the anolyte and catholyte solutions and combined, and the fluoride content for these combined samples was determined as per the general method in Section 2.6. These results were then compared with those obtained for the performance of the conventional proton exchange membrane electrolyser as shown in Fig. 6A and B (the latter of which shows the rate of fluoride production normalised to the active area of the membrane electrode assembly). These results demonstrate that the release of fluoride is at least an order of magnitude lower in the ECPB-mediated system than in the conventional proton exchange membrane electrolyser over this timescale, suggesting that an ECPB-mediated system might indeed reduce membrane degradation *via* attack of reactive oxygen species.

4. Conclusions

In summary, we have demonstrated the operation of an electrolyser using silicotungstic acid as an electron-coupled-proton buffer where complete decoupling of the oxygen evolution and hydrogen evolution reactions can be achieved at current densities of up to 500 mA cm^{-2} under steady state conditions. This allowed O_2 and H_2 to be produced continuously, and demonstrates that this electron-coupled-proton buffer can be cycled numerous times in any given experiment. The ECPB-mediated electrolyser was able to produce oxygen with under 0.4% hydrogen contamination at current densities as low as 25 mA cm^{-2}, in contrast to the abilities of a conventional proton exchange membrane electrolyser built using similar components. Moreover, we have shown that an electrolysis device containing a silicotungstic acid ECPB is potentially more tolerant of mineralised water inputs than a conventional proton exchange membrane electrolyser, and also that fluoride release from the perfluorosulfonated membrane (a marker for membrane

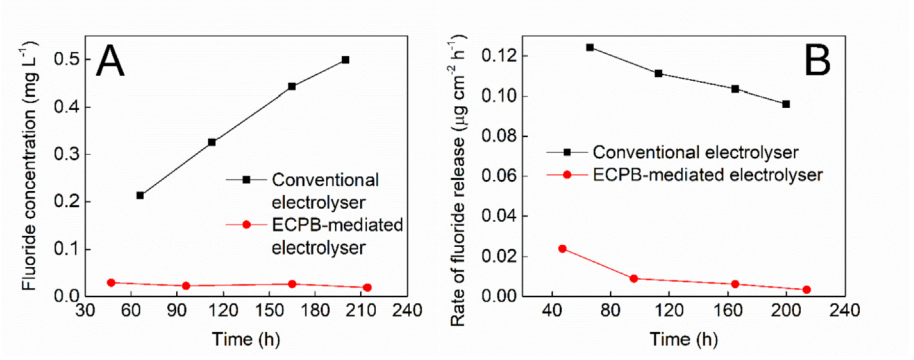

Fig. 6. A: Fluoride concentration in solution as a function of time for a conventional electrolyser (black line and squares) and an ECPB-mediated electrolyser (red line and circles). 6B: Rate of fluoride release as a function of time for a conventional electrolyser (black line and squares) and an ECPB-mediated electrolyser (red line and circles).

degradation) is lower in an ECPB-mediated cell than in a conventional proton exchange membrane electrolyser. This work thus serves to highlight the potential advantages of using silicotungstic acid as an electron-coupled-proton buffer for electrolysis over a wide range of current densities, with implications for harnessing renewably-generated power for hydrogen production.

Acknowledgments

MDS thanks the Royal Society for a University Research Fellowship (UF150104). This work was supported by the EPSRC (EP/K023004/1 and EP/R020914/1) and Scottish Enterprise (SPO156134). The data underpinning this work are available at https://doi.org/10.5525/gla.researchdata.905.

References

[1] I. Roger, M.A. Shipman, M.D. Symes, Earth-abundant catalysts for electrochemical and photoelectrochemical water splitting, Nat. Rev. Chem. 1 (2017), 0003.
[2] N.S. Lewis, D.G. Nocera, Powering the planet: chemical challenges in solar energy utilization, Proc. Natl. Acad. Sci. U.S.A. 103 (2006) 15729–15735.
[3] B. You, Y. Sun, Innovative strategies for electrocatalytic water splitting, Acc. Chem. Res. 51 (2018) 1571–1580.
[4] N. Armaroli, V. Balzani, The hydrogen issue, ChemSusChem 4 (2011) 21–36.
[5] E.L. Miller, D. Papageorgopoulos, N. Stetson, K. Randolph, D. Peterson, K. Cierpik-Gold, A. Wilson, V. Trejos, J.C. Gomez, N. Rustagi, S. Satyapal, U.S. Department of energy hydrogen and fuel cells program: progress, challenges and future directions, MRS Adv 1 (2016) 2839–2855.
[6] F. Le Formal, W.S. Bourée, M.S. Prévot, K. Sivula, Challenges towards economic fuel generation from renewable electricity: the need for efficient electrocatalysis, Chimia 69 (2015) 789–798.
[7] J.D. Holladay, J. Hu, D.L. King, Y. Wang, An overview of hydrogen production technologies, Catal. Today 139 (2009) 244–260.
[8] M. Carmo, D.L. Fritz, J. Mergel, D. Stolten, A comprehensive review on PEM water electrolysis, Int. J. Hydrogen Energy 38 (2013) 4901–4934.
[9] M.D. Symes, Just add hot water, Nat. Energy 4 (2019) 730–731.
[10] F. Barbir, PEM electrolysis for production of hydrogen from renewable energy sources, Sol. Energy 78 (2005) 661–669.
[11] L. Ghassemzadeh, K.-D. Kreuer, J. Maier, K. Müller, Chemical degradation of nafion membranes under mimic fuel cell conditions as investigated by solid-state NMR spectroscopy, J. Phys. Chem. C 114 (2010) 14635–14645.
[12] V. Prabhakaran, C.G. Arges, V. Ramani, Investigation of polymer electrolyte membrane chemical degradation and degradation mitigation using in situ fluorescence spectroscopy, Proc. Natl. Acad. Sci. U.S.A. 109 (2012) 1029–1034.
[13] T.E. Mallouk, Divide and conquer, Nat. Chem. 5 (2013) 362–363.
[14] A.G. Wallace, M.D. Symes, Decoupling strategies in electrochemical water splitting and beyond, Joule 2 (2018) 1390–1395.
[15] X. Liu, J. Chi, B. Dong, Y. Sun, Recent progress in decoupled H_2 and O_2 production from electrolytic water splitting, ChemElectroChem 6 (2019) 2157–2166.
[16] M.D. Symes, L. Cronin, Decoupling hydrogen and oxygen evolution during electrolytic water splitting using an electron-coupled-proton buffer, Nat. Chem. 5 (2013) 403–409.
[17] B. Rausch, M.D. Symes, G. Chisholm, L. Cronin, Decoupled catalytic hydrogen evolution from a molecular metal oxide redox mediator in water splitting, Science 345 (2014) 1326–1330.
[18] B. Rausch, M.D. Symes, L. Cronin, A bio-inspired, small molecule electron-coupled-proton buffer for decoupling the half-reactions of electrolytic water splitting, J. Am. Chem. Soc. 135 (2013) 13656–13659.
[19] L.G. Bloor, R. Solarska, K. Bienkowski, P.J. Kulesza, J. Augustynski, M.D. Symes, L. Cronin, Solar-driven water oxidation and decoupled hydrogen production mediated by an electron-coupled-proton buffer, J. Am. Chem. Soc. 138 (2016) 6707–6710.
[20] L. MacDonald, J.C. McGlynn, N. Irvine, I. Alshibane, L.G. Bloor, B. Rausch, J.S.J. Hargreaves, L. Cronin, Using earth abundant materials for the catalytic evolution of hydrogen from electron-coupled proton buffers, Sustainable Energy Fuels 1 (2017) 1782–1787.
[21] L. MacDonald, B. Rausch, M.D. Symes, L. Cronin, Selective hydrogenation of nitroarenes using an electrogenerated polyoxometalate redox mediator, Chem. Commun. 54 (2018) 1093–1096.
[22] N. Kirkaldy, G. Chisholm, J.-J. Chen, L. Cronin, A practical, organic-mediated, hybrid electrolyser that decouples hydrogen production at high current densities, Chem. Sci. 9 (2018) 1621–1626.
[23] J.J. Chen, M.D. Symes, L. Cronin, Highly reduced and protonated aqueous solutions of $[P_2W_{18}O_{62}]^{6-}$ for on-demand hydrogen generation and energy storage, Nat. Chem. 10 (2018) 1042–1047.
[24] J. Lei, J.-J. Yang, T. Liu, R.-M. Yuan, D.-R. Deng, M.-S. Zheng, J.-J. Chen, L. Cronin, Q.-F. Dong, Tuning redox active polyoxometalates for efficient electron-coupled proton-buffer-mediated water splitting, Chem. Eur J. 25 (2019) 11432–11436.
[25] V. Amstutz, K.E. Toghill, F. Powlesland, H. Vrubel, C. Comninellis, X. Hu, H.H. Girault, Renewable hydrogen generation from a dual-circuit redox flow battery, Energy Environ. Sci. 7 (2014) 2350–2358.
[26] P. Peljo, H. Vrubel, V. Amstutz, J. Pandard, J. Morgado, A. Santasalo-Aarnio, D. Lloyd, F. Gumy, C.R. Dennison, K.E. Toghill, H.H. Girault, All-vanadium dual circuit redox flow battery for renewable hydrogen generation and desulfurisation, Green Chem. 18 (2016) 1785–1797.
[27] B. You, X. Liu, N. Jiang, Y. Sun, A general strategy for decoupled hydrogen production from water splitting by integrating oxidative biomass valorization, J. Am. Chem. Soc. 138 (2016) 13639–13646.
[28] F. Li, F. Yu, J. Du, Y. Wang, Y. Zhu, X. Li, L. Sun, Water splitting via decoupled photocatalytic water oxidation and electrochemical proton reduction mediated by electron-coupled-proton buffer, Chem. Asian J. 12 (2017) 2666–2669.
[29] W. Li, N. Jiang, B. Hu, X. Liu, F. Song, G. Han, T.J. Jordan, T.B. Hanson, T.L. Liu, Y. Sun, Electrolyzer design for flexible decoupled water splitting and organic upgrading with electron reservoirs, Chem 4 (2018) 637–649.
[30] A. Landman, H. Dotan, G.E. Shter, M. Wullenkord, A. Houaijia, A. Maljusch, G.S. Grader, A. Rothschild, Photoelectrochemical water splitting in separate oxygen and hydrogen cells, Nat. Mater. 16 (2017) 646–651.
[31] L. Chen, X. Dong, Y. Wang, Y. Xia, Separating hydrogen and oxygen evolution in alkaline water electrolysis using nickel hydroxide, Nat. Commun. 7 (2016) 11741.
[32] Z. Jin, P. Li, D. Xiao, A hydrogen-evolving hybrid-electrolyte battery with electrochemical/photoelectrochemical charging from water oxidation, ChemSusChem 10 (2017) 483–488.
[33] Y. Ma, X. Dong, Y. Wang, Y. Xia, Decoupling hydrogen and oxygen production in acidic water electrolysis using a polytriphenylamine-based battery electrode, Angew. Chem. Int. Ed. 57 (2018) 2904–2908.
[34] S. Goodwin, D.A. Walsh, Closed bipolar electrodes for spatial separation of H_2 and O_2 evolution during water electrolysis and the development of high-voltage fuel cells, ACS Appl. Mater. Interfaces 9 (2017) 23654–23661.
[35] W. Wu, X.-Y. Wu, S.-S. Wang, C.-Z. Lu, Highly efficient hydrogen evolution from water electrolysis using nanocrystalline transition metal phosphide catalysts, RSC Adv. 8 (2018) 39291–39295.
[36] Y. Ma, Z. Guo, X. Dong, Y. Wang, Y. Xia, Organic proton-buffer-electrode to separate hydrogen and oxygen evolution in acid water electrolysis, Angew. Chem. Int. Ed. 58 (2019) 4622–4626.
[37] A. Ho, X. Zhou, L. Han, I. Sullivan, C. Karp, N.S. Lewis, C. Xiang, Decoupling $H_2(g)$ and $O_2(g)$ production in water splitting by a solar-driven $V^{3+/2+}(aq,H_2SO_4)|KOH(aq)$ cell, ACS Energy Lett 4 (2019) 968–976.
[38] P. Belleville, F. Guillet, A. Pons, J. Deseure, G. Merlin, F. Druart, J. Ramousse, E. Grindler, Low voltage water electrolysis: decoupling hydrogen production using bioelectrochemical system, Int. J. Hydrogen Energy 43 (2018) 14867–14875.
[39] J. Wang, L. Ji, X. Teng, Y. Liu, L. Guo, Z. Chen, Decoupling half-reactions of electrolytic water splitting by integrating a polyaniline electrode, J. Mater. Chem. 7 (2019) 13149–13153.
[40] H. Dotan, A. Landman, S.W. Sheehan, K.D. Malviya, G.E. Shter, D.A. Grave, Z. Arzi, N. Yehudai, M. Halabi, N. Gal, N. Hadari, C. Cohen, A. Rothschild, G.S. Grader, Decoupled hydrogen and oxygen evolution by a two-step electrochemical–chemical cycle for efficient overall water splitting, Nat. Energy 4 (2019) 786–795.
[41] B. Keita, L. Nadjo, New aspects of the electrochemistry of heteropolyacids: Part II. Coupled electron and proton transfers in the reduction of silicoungstic species, J. Electroanal. Chem. 217 (1987) 287–304.
[42] N. Mamaca, E. Mayousse, S. Arrii-Clacens, T.W. Napporn, K. Servat, N. Guillet, K.B. Kokoh, Electrochemical activity of ruthenium and iridium based catalysts for oxygen evolution reaction, Appl. Catal., B 111–112 (2012) 376–380.
[43] S. Siracusano, V. Baglio, N. Briguglio, G. Brunaccini, A. Di Blasi, A. Stassi, R. Ornelas, E. Trifoni, V. Antonucci, A.S. Aricò, An electrochemical study of a PEM stack for water electrolysis, Int. J. Hydrogen Energy 37 (2012) 1939–1946.
[44] P. Millet, R. Ngameni, S.A. Grigoriev, N. Mbemba, F. Brisset, A. Ranjbari, C. Etiévant, PEM water electrolyzers: from electrocatalysis to stack development, Int. J. Hydrogen Energy 35 (2010) 5043–5052.
[45] See, for example, Installation Permitting Guidance for Hydrogen and Fuel Cell Stationary Applications: UK Version, Health and Safety Laboratory, Derbyshire, UK, 2009. Accessed, http://www.hse.gov.uk/research/rrpdf/rr715.pdf. (Accessed September 2019).
[46] F. Andolfatto, R. Durand, A. Michas, P. Millet, P. Stevens, Solid polymer electrolyte water electrolysis: electrocatalysis and long-term stability, Int. J. Hydrogen Energy 19 (1994) 421–427.
[47] M. Aoki, H. Uchida, M. Watanabe, Novel evaluation method for degradation rate of polymer electrolytes in fuel cells, Electrochem. Commun. 7 (2005) 1434–1438.
[48] M. Aoki, H. Uchida, M. Watanabe, Decomposition mechanism of perfluorosulfonic acid electrolyte in polymer electrolyte fuel cells, Electrochem. Commun. 8 (2006) 1509–1513.
[49] V.O. Mittal, H.R. Kunz, J.M. Fenton, Is H_2O_2 involved in the membrane degradation mechanism in PEMFC? Electrochem. Solid State Lett. 9 (2006) A299–A302.
[50] S. Kundu, M.W. Fowler, L.C. Simon, R. Abouatallah, N. Beydokhti, Degradation analysis and modeling of reinforced catalyst coated membranes operated under OCV conditions, J. Power Sources 183 (2008) 619–628.